Hindawi
International Journal of Photoenergy
Volume 2021, Article ID 6679576, 22 pages
https://doi.org/10.1155/2021/6679576

Research Article

Biaxial Equatorial Solar Tracker with High Precision and Low Consumption: Modelling and Realization

Hicham Bouzakri, Ahmed Abbou, Khalil Tijani, and Zakaria Abousserhane

Electrical Engineering Department, Mohammadia School of Engineers, Mohammed V University in Rabat, Morocco

Correspondence should be addressed to Hicham Bouzakri; hichambouzakri@research.emi.ac.ma

Received 11 October 2020; Revised 26 January 2021; Accepted 3 March 2021; Published 19 March 2021

Academic Editor: Alberto Álvarez-Gallegos

The solar tracker is a mechanism that helps the photovoltaic panel to maximize its performance, while keeping it oriented towards direct solar radiation. In order to specify tracking, most solar trackers use two axes, one horizontal and the other vertical, which implies an increase of the consumed energy and a decrease in precision, since we have to make both motors operate simultaneously. This paper is a modelling of a biaxial solar tracker, with the principle of an equatorial mount, allowing it to precisely follow the sun via a single axis (equatorial axis), while the second axis (tilt axis) makes a small daily correction of few seconds at sunrise. In this way, our model keeps precision to the maximum, with minimum energy consumption. A detailed simulation clearly shows that the proposed model receives the maximum solar irradiation that a normal surface to solar radiation can receive and may in a certain period of the year receive a gain in the amount of solar irradiation; we have up to 63.47% compared to a fixed installation. The study details the different tracking methods, in order to adapt the concept model to the type of solar panel used. We closed finish the study with the realization of the prototype with a detailed explanation of the concept movement. To validate the simulation, we have made an experience that gives us the same results as given by simulation.

1. Introduction

Renewable energy is the production of energy from an unlimited source, such as the sun's rays, or the wind. Since 2009, Morocco has adopted a strategy based on strengthening energy efficiency by the integration of renewable energies. Photovoltaic solar energy is among the energies used on a large scale, which allows the production of electricity from solar radiation. The yield is therefore essentially linked to the amount of solar radiation absorbed by the photovoltaic cells [1, 2]. The solar tracker is a mechanism introduced to the photovoltaic panel which allows it to be permanently oriented to direct solar radiation from sunrise to sunset. As long as there is a precise tracking, there will be a maximum of absorbed solar radiation, and then, the photovoltaic panel will operate at its maximum efficiency. Based on this principle, many studies and research have been carried out in order to approach maximum efficiency with minimum energy consumption, since the solar tracker also takes a significant part of the electric power which comes from the photovoltaic panel. We can therefore distinguish between two types of solar trackers: A monoaxial solar tracker [3–5]. A biaxial solar tracker [6–8].

A study and realization done by researchers in Greece of a solar tracker with double axes, horizontal and vertical, found an increase in solar radiation of 19.1% to 30.2% depending on the season. They chose to use open-loop tracking without a solar collector, which minimized the cost of production [9]. In the same trend, a new strategy for a two-axis tracking system was devised by researchers in China. They proposed the open loop to control and adapt the tracking frequency at all times; according to them, this manipulation improves tracking precision and therefore increase the yield [10]. Another achievement was made in Thailand by researchers who designed a two-axis solar tracker with a closed-loop tracking strategy. They found a 44.89% increase

in energy efficiency [11]. An experimental study carried out by researchers in Greece showed an increase in electrical power gain of photovoltaic panel with tracking system compared to the one in fixed mode; the results show an increase of 37.1% for two-axis trackers; this gain is distributed over the seasons as a result; we observe 33.6% in spring, 43.6% in summer, 38.3% in autumn, and 28.8% in winter [12]. Another comparison study between different types of solar trackers has been carried out by researchers in India, which shows that a biaxial solar tracker offers more precision (therefore more efficiency) than the one with a single axis, while a single-axis tracker consumes less electrical energy and contains a complex control mechanism than the one with two axes [13].

The common point between previous researches is the use of solar trackers with two horizontal and vertical axes, while the sun makes an apparent circular path around the polar star. So in all these researches, we had to vary the two axes simultaneously and therefore do the follow-up control on the two axes at the same time, which will complicate the precision and of course will increase the system consumption. Using single-axis tracker reduces energy consumption, but it also reduces the level of precision. In case we are going to use a concentrated photovoltaic panel (LCPV or HCPV), a single-axis tracking will be almost impossible. The tracking method in these studies switches between the open loop and the closed loop; sometimes researchers decide to combine between the two methods. It is true that an open-loop solar tracker increases accuracy if we have a model suitable enough for tracking with a good programming strategy, but this method is a waste of energy for overcast sites. Also in all the previous researches, the problem of strong wind was not treated. A strong wind will probably damage the solar tracker structure.

The research that we carried out before proposes models of solar trackers capable of maintaining the maximum yield with the minimum consumption. In 2019, in a conference held in Agadir (Morocco), we proposed a model of a monoaxial solar tracker with an equatorial mount, which allows the photovoltaic panel to have a precise tracking of the sun with a single axis and therefore a single motor. This study showed us that the yield of the photovoltaic panel remains at maximum from sunrise to sunset during the periods close to the equinoxes (March 20/21 and September 22/23) and decreases up to 91.3% in periods close to the solstices (the winter solstice on December 21/22 and summer solstice on June 20/21) [14]. In 2020, we proposed via a detailed study an improvement of the previous model with a reflection system, so that it can keep the yield of the photovoltaic panel at its maximum throughout the year [15]. These two studies and realizations take into consideration the circular trajectory of the sun around the pole star (apparent trajectory) and show that with a single motor, we can make a perfect follow-up of the sun and gather a quantity of direct solar radiation which keeps the maximum efficiency of the photovoltaic panel. The disadvantage is that these models are valid only with a photovoltaic panel without concentration, while if we are going to use a photovoltaic module with concentration (LCPV or HCPV), we will be forced to vary the inclination of the solar panel following the daily variation of the solar declination. Also, a monoaxial model remains fragile against a strong wind speed.

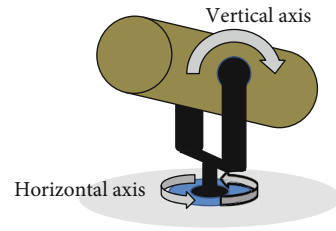

Figure 1: The telescope on an azimuth mount.

This paper proposes a biaxial solar tracker with the principle of an equatorial mount which will be valid for all kinds of photovoltaic panels (PV, LCPV, and HCPV) while keeping their maximum performance throughout the year with a minimum consumption of energy. The advantage of this model is that it will have high precision with an acceptance angle equal to or less than 1°, which allows the photovoltaic cells with concentration to keep the perfect focus of direct solar radiation throughout the day. The tracking will be with a single axis called the equatorial axis (which minimizes consumption), while the second axis called the tilt axis will correct the tilt of the panel only at sunrise (the tilt motor works for few minutes at sunrise). The equatorial axis tracking will be in a closed loop via a simple LDR sensor and the daily tilt correction will be in an open loop. The concept takes into account the problem of strong wind, which will be solved by putting the panel in horizontal oriented towards the zenith (the parking mode).

The study begins with the explanation of the principle and operation of an equatorial mount, and then, we will introduce this principle in the proposed concept, in order to model a biaxial solar tracker suitable for all types of photovoltaic panel (PV, LCPV, and HCPV). In order to valorize our work, we will do a comparison by simulating three modes of installation of a photovoltaic solar tracking system: the first is in fixed mode, the second is in biaxial azimuthal tracking mode (followed by two horizontal and vertical axes), while the third is in two-axis equatorial tracking mode (the proposed model). The next chapter will be a detailed study of the main method by which we will track and correct the tilt. Finally, we will complete the study by the realization of the prototype in order to be valorized experimentally.

2. The Azimuth Mount and the Equatorial Mount

An azimuthal mount is a motorized mechanism used for tracking celestial bodies (stars, planets, moon, sun, etc.) based on the variation of two axes simultaneously horizontal and vertical. An azimuthal mount can be illustrated as shown in Figure 1 is widely used for telescopes [16].

The disadvantage of this type of mount is that you have to vary the two axes simultaneously in order to follow the star perfectly and, therefore, have the two motors activated at the same time. This implies a high energy consumption since

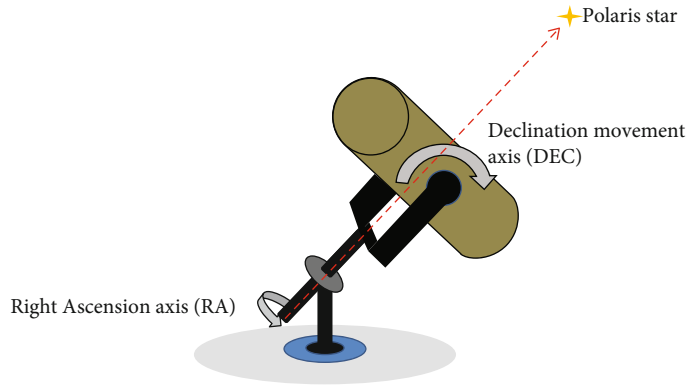

Figure 2: The telescope on an equatorial mount.

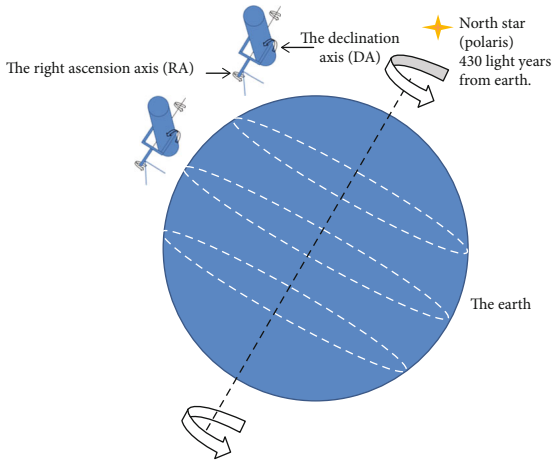

Figure 3: The telescope tracking axis is parallel to the earth's axis of rotation.

the majority of energy is consumed by the motors, also making tracking accuracy complicated.

It is for this reason that telescopes that form the basis of astrophotography or research use a more suitable mechanism called the equatorial mount [16]. An equatorial mount, as shown in Figure 2, is a mechanism that allows the telescope to follow the objects on the sky (stars, planets, moon, sun, etc.) with a single axis called "Right Ascension RA" [16]. According to Figures 3 and 4, the principle is simple, since the earth rotates around itself in 24 hours on the north-south axis of rotation (the earth's axis of rotation) and that this axis is almost oriented towards the North Star (the North Star at a distance of 430 light years from the earth), all the objects of the sky (stars, sun, lunar, planets, galaxies, nebula, etc.) seem to revolve around it. So to make a perfect follow-up, it is enough to orient the follow-up axis towards the pole star. In this way, only one motor is activated during the follow-up [16].

The main advantage of this type of mount is the precision of the tracking and the minimum energy consumption.

In order to keep the photovoltaic panel oriented perpendicular to direct solar radiation, the majority of solar trackers use an azimuth mount and, therefore, follow the apparent path of the sun via two horizontal and vertical axes (Figure 5).

In order to perfectly follow the sun, the system operates both motors simultaneously horizontally and vertically, which makes the cascade tracking movement as shown in Figure 6 as a consequence this will complicate tracking and increase system energy consumption.

In the case of using a concentration or a high concentration photovoltaic panel (LCPV or HCPV), the notion of precision will be of great importance, since this kind of solar panel has a concentration system which focuses direct solar radiation on top of cells. The goal as shown in Figures 7 and 8 is to introduce the principle of the equatorial mount to the solar tracker, in order to minimize energy consumption and increase tracking accuracy, thus using a single motor during tracking.

3. Solar Declination

According to Figures 9 and 10, we all know that the earth rotates around the sun in 356 days and 6 hours and that its axis of rotation is inclined at 66.55° relative to the earth's orbital plane [17].

The apparent solar path in the sky seems to be deviating every day. It lies from the winter solstice to the summer solstice passing through the equinox and, then, descends to the winter solstice (Figure 11). This is the solar declination [17].

This declination angle is calculated by the following relationship [17]:

$$\delta = 23.45 \sin\left[\frac{360}{365}(d_n + 284)\right] \text{ in degree,} \quad (1)$$

with d_n day number of year, 1 on 1 January and 365 on 31 December.

The solar declination angle δ is cancelled at the equinoxes and equal to +23.45° at the summer solstice and -23.45° at the winter solstice [17]. To correct this variation, our solar tracker as shown in Figure 12 will be biaxial. The first axis is devoted to equatorial tracking (always oriented towards the North Star), the second to the solar declination which is varied only once a day.

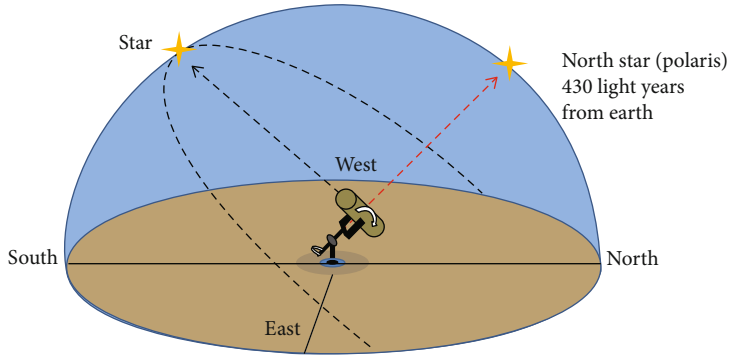

Figure 4: The tracking a telescope on an equatorial mount.

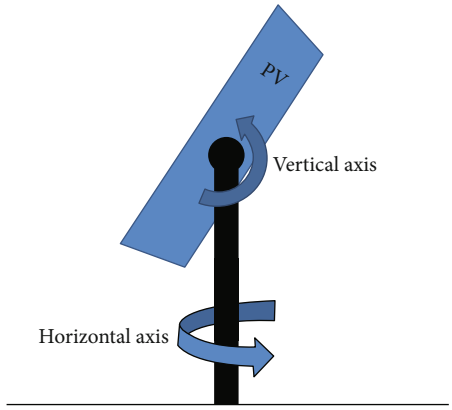

Figure 5: A photovoltaic panel on an azimuth mount.

At sunrise, the system adapts the tilt axis to the day's solar declination angle, and then, it switches to tracking via a single axis (the tracking axis).

In this way, there will be only one motor activated during tracking; the other will only run for a few minutes at sunrise and, therefore, minimize consumption and increase system accuracy.

4. The Concept Proposed

For a better orientation of the tracking axis towards the polar star, we used a hollow iron tube (Figure 13), thus making it possible to orient it precisely at the polar star.

According to Figure 14, the tracking axis will be fixed through two bearings with a mechanism that can be moved in two directions, horizontal and vertical, thus facilitating the stationing. After correcting the orientation of this axis, the mechanism is fixed with hexes nuts. The inclination axis will be fixed perpendicular to the tracking axis, thus giving the possibility of correcting the inclination of the panels according to the solar declination (a daily correction). This axis was also fixed with a support via two bearings (Figure 15).

In order to have a good balance, the solar panels will be distributed to the left and right of the tilt axis (Figures 16 and 17). In the case of a single panel, it can be fixed directly to this axis.

5. The Simulation

In order to enhance the proposed model, we will do a simulation using the PVSYST software. We have chosen the city of Khemisset in Morocco as a site simulation with the following coordinates:

Latitude = 33.838°
Longitude = -6.083°
Altitude = 458 m

The PV panel chosen for the simulation is as the type below: Mono 50 Wp 36 cells (PV Array design = 1 Modules).

Since a fixed installation of a photovoltaic panel is a benchmark for any tracking model. The first simulation will be in fixed mode with a south orientation and an inclination equal to the latitude of the place (33.8° for our study case) (Figure 18).

The second simulation will be with a tracking system using two axes (horizontal and vertical), and it is the most used model for sun's tracking (Figure 19).

The proposed model is presented on the third simulation, which is a biaxial equatorial tracking (Figure 20).

The tracking axis is oriented through polar star (or to the north with an inclination equal to the latitude of the site). While the second axis named the inclination, enable the PV panel to change its inclination while keeping the tracking axis always oriented to the Polaris.

"Axis tilt" = latitude of place (33.8° for Khemisset city).

"Axis azimuth" = 0° the South-Nord tracking axis.

"Frame Phi min" = -90° and "Frame Phi max" = 90° the tracking between east and west.

"Min. tilt/frame" and "Max. tilt/frame" are the minimum and maximum of the variation of the panel tilt axis.

Normally, we should introduce to the <<min. tilt/-frame>> the minimal panel's inclination (-23.45° when the sun is on the summer solstice see Figure 11) and the <<max. tilt/frame>> the maximal panel's inclination(+23.45° when the sun is on the winter solstice see Figure 11); then, we have done a batch simulation (by performing the simulation for different tilt angle) to see the output in terms of irradiation for each degree tilt between -23° and +23°.

The same thing will be done for the three models to make a comparison at the end.

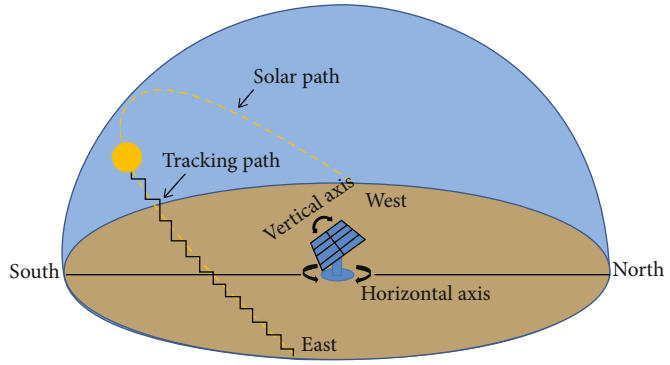

Figure 6: The cascading path of the azimuthal solar tracker movement.

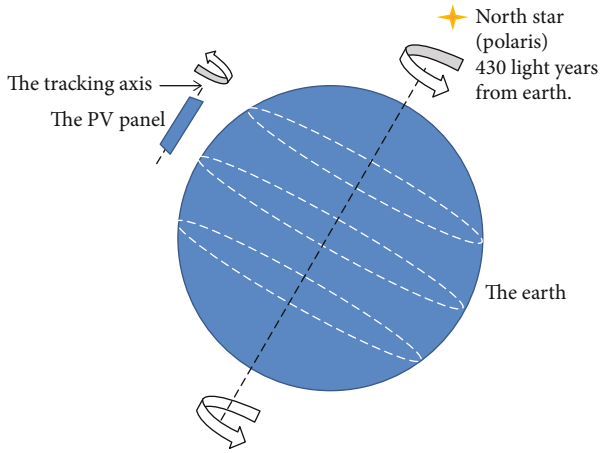

Figure 7: The solar panel tracking axis is parallel to the earth's axis of rotation.

For example, between 18 and 21 of Mai, the solar declination is a median of 20°; then, min. tilt/frame = 20° and max. tilt/frame = 20°.

Reported to Equation (1), we can extract days of the year for each inclination degree between -23° and +23°, and we will perform the simulation for each model and each period, taking into consideration the variation of min. tilt/frame and max. tilt/frame for the third simulation.

Column 1: the period (calculated by Equation (1)).

Column 2: the solar declination δ in degrees, so then min. tilt/frame = max. tilt/frame = $-\delta$ (Figure 21).

Column 3: the amount of incident solar irradiation for a panel in fixed mode (kWh/m^2).

Column 4: the amount of incident solar irradiation for a panel with a horizontal and vertical dual-axis tracker (kWh/m^2).

Column 5: the amount of incident solar irradiation for a panel with an equatorial two-axis tracker (kWh/m^2).

Column 6: the percentage gain of the equatorial biaxial model compared to the fixed model.

6. Results and Discussion

According to Tables 1–4, the main parameter to take into consideration in the previous simulation is the quantity of the received irradiation that beams on the panel's surface. This quantity is different for each type of installation; this is due to the DNI (Direct Normal Irradiation) which is the predominant one.

We can remark clearly that the quantity of the incidence solar irradiation with a two axes solar tracking horizontal and vertical is approximately equal to the one received by our proposed model.

For the fixed installation, the quantity of the global irradiation is 2147.19 kWh/m^2, while with a biaxial equatorial tracking system, we will have 2917.65 kWh/m^2 (an increase of 35.88%).

We can also remark a gain in certain days in the year that overpass 60% (63.47% between 21 June and 06 July Table 2), and this percentage will change with seasons (the gain during summer and spring is higher than the one during autumn and winter). During the simulation, the variation of the panel's inclination is done with an increment of one degree, while the real proposed model change constantly the panel's inclination, which can without any doubt absorb more solar irradiation than the one absorbed by an azimuthal two-axis tracking system.

7. The Motorization of the Concept

The proposed concept contains two axes, the tilt axis and the equatorial axis. So, two motors must be used, one on the equatorial axis (the tracking axis), the other on the tilt axis. In order to minimize power consumption and increase accuracy, we opted for a stepper motor. We all know that a stepper motor is a low torque motor. We will therefore add a high torque reduction gear to support a set of photovoltaic modules. Figures 22–24 represent the proposed reducer, it is the worm type combined with a pinion reducer.

7.1. The Tracking Axis. The tracking axis is the axis that allows the mechanism to track the sun during the day. There are two tracking methods:

(i) Scheduled tracking or open loop

(ii) Tracking by sensor or closed loop

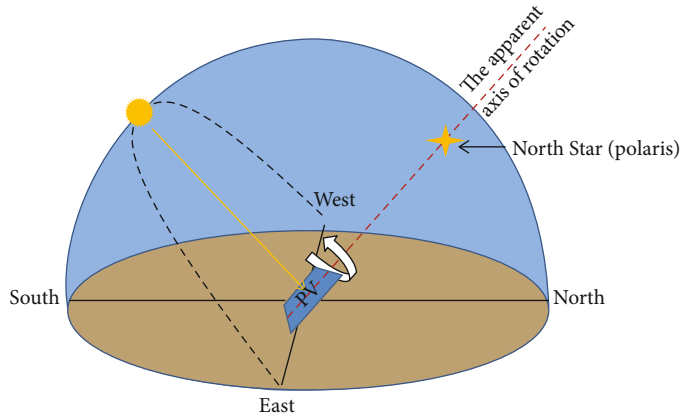

Figure 8: The solar tracker on an equatorial mount.

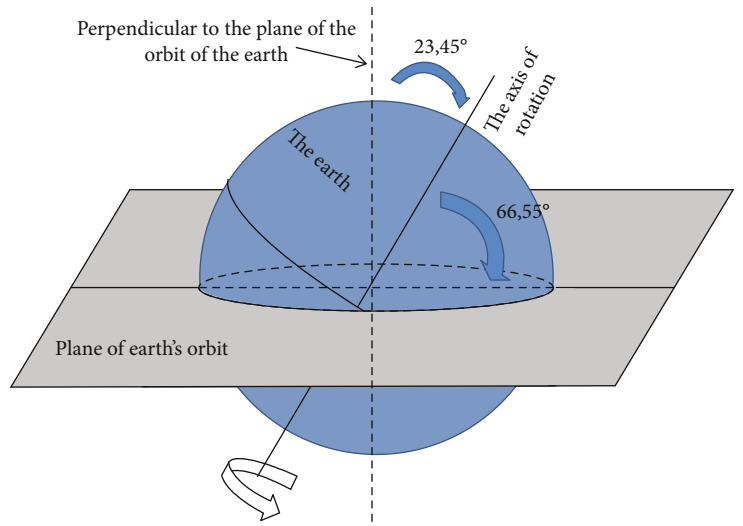

Figure 9: The inclination of the axis of rotation with respect to the plane of the earth's orbit.

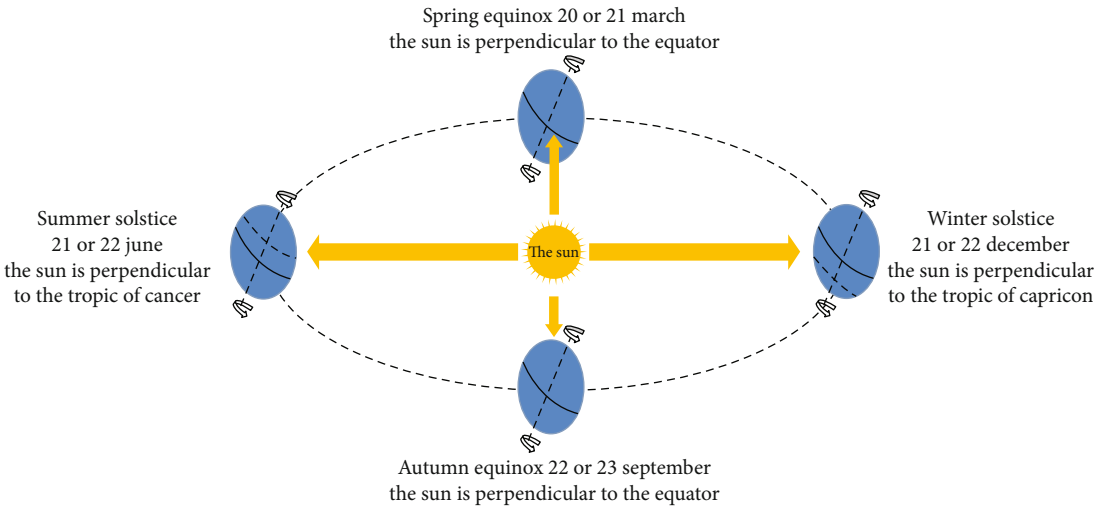

Figure 10: Movement of the earth around the sun.

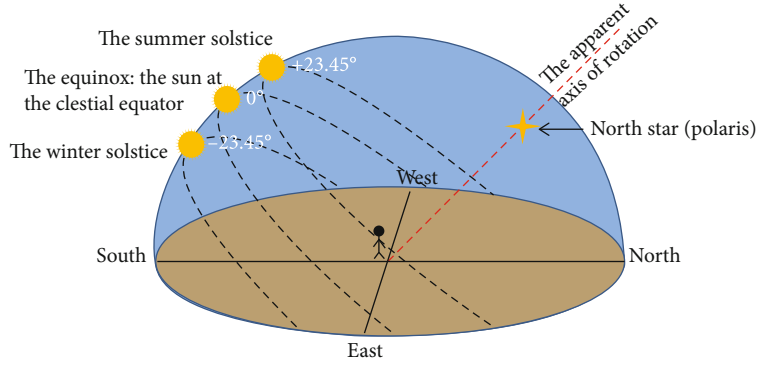

Figure 11: The angle of solar declination.

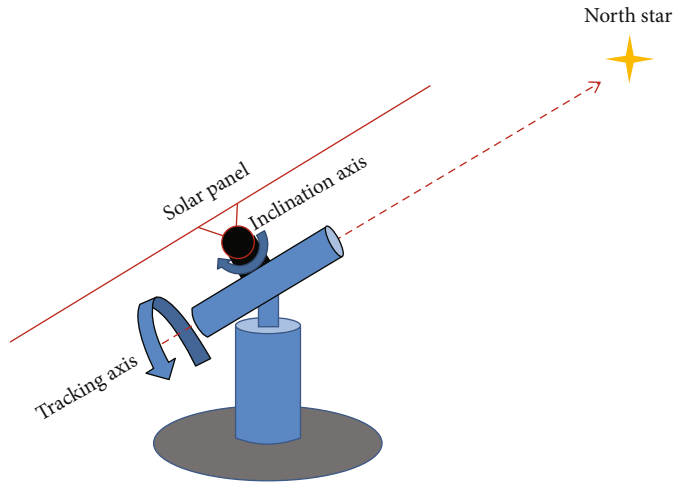

Figure 12: Two-axis solar tracker on an equatorial mount.

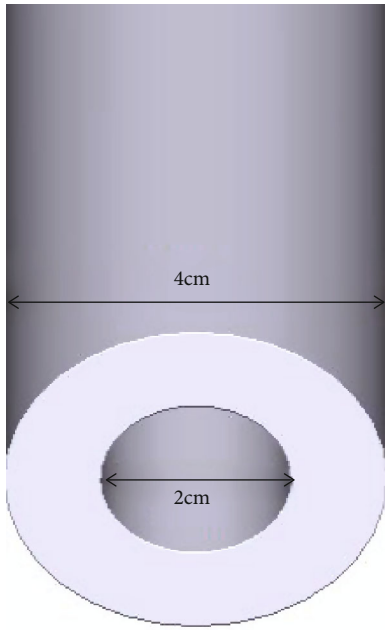

Figure 13: The tracking axis in the form of a hollow tube.

7.1.1. Scheduled Tracking. Scheduled tracking is the open-loop tracking, which involves tracking the sun blindly, that is to say this axis must rotate at the apparent speed of the sun's movement during the day. We know that a day averages 24 hours (86400 s), so the apparent angular speed of the sun's movement is the following:

$$\omega_s = 2\pi/86400\text{s} \simeq 7.27 \times 10^{-5}\ \text{rad}/s \quad (2)$$

So the tracking axis must rotate at the same speed in order to follow this apparent movement of the sun. And since this axis has a coupler that is at the same time a reducer, the speed of the motor at the input of the reducer will be

$$\omega_s/\text{reduction rate} \quad (3)$$

Our reducer used is of the "DiseqC motor" type with a reduction rate of 1/6000 (Figure 25). So the angular speed of the motor must be (Figure 26):

$$\omega_m = \omega_s \times 6000 = 4.36\ \text{rad}/s \quad (4)$$

7.1.2. Sensor Tracking. Tracking with the solar captor is closed-loop tracking, which consists of using a solar position sensor. Following the data received by this sensor, the system

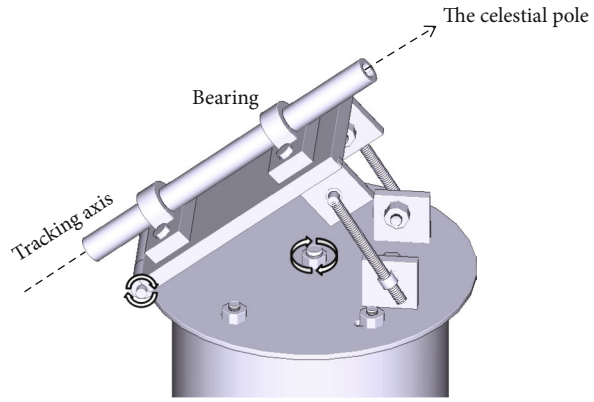

Figure 14: The tracking axis maintained with a mechanism.

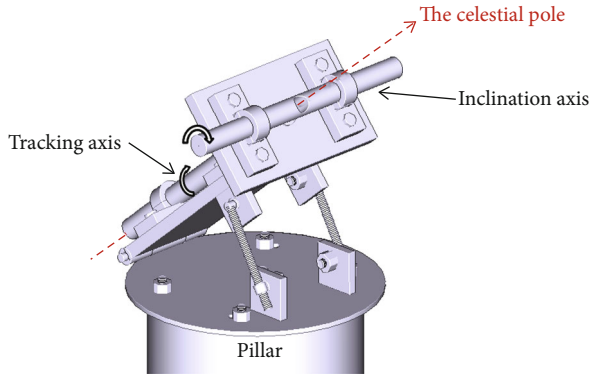

Figure 15: The equatorial mount with the tracking axis and the tilt axis.

activates the tracking motor to track in east or west orientation, in order to keep the panels facing the sun's rays directly. There are several models of solar collectors; the simplest among them are those using LDR. The sensor proposed for our tracking axis is presented in Figure 27; this sensor is based on 3 LDR with two walls; one separates the 1st LDR from the 2nd, and the second wall separates the 2nd LDR from the 3rd. The height of the wall is calculated according to the acceptance angle α chosen.

According to Figures 28 and 29, the length of the wall AB is related to the width of the LDR (4 mm) and the acceptance angle α.

$$\text{So}: \text{AB} = \text{BC}/\sin \propto = 4\text{mm}/\sin \propto \quad (5)$$

From Equation (5) and with an acceptance angle equal to 1°, the length of the wall must be 23 cm (as long as the length of the wall is increased the accuracy of the sensor increases). If $\alpha > 1°$ the LDR 2 is in total darkness, the LDR1 is in lit. This sensor is a monoaxial sensor, which means that it gives us the position of the sun in a single axis and which is the equatorial axis. However, the sun changes its inclination during year between -23.45° and +23.45°. It is for this reason that we must also calculate the width of the walls (Figures 29 and 30).

According to Figure 29, we have

$$w = \tan(23.45°) \times \text{L} \quad (6)$$

If $L = 23$ cm, so $w = 10$ cm.

Since the open-loop tracking is done independently to the state of the sky (clear or cloudy), which implies a loss of energy consumed by the tracker especially if the sky was covered for days, we then decided to use closed-loop tracking. So tracking will only be active if LED2 is completely obscured.

We all know that the resistance of an LDR varies with the brightness; it decreases as long as the LDR is lit. In this case, we will use an assembly based on the voltage divider rule as shown in Figure 31. Each LDR is connected in series with a resistance of 10 k. The circuit is supplied with 5 v, and the output will be at the LDR terminal.

$$V_{\text{output}} = 5\text{v} \times \left(\frac{R_{\text{LDR}}}{R_{\text{LDR}} + R}\right) \quad (7)$$

From Equation (7), if we are in night mode the LDR is in total darkness, so its resistance tends to infinity, then $V_{\text{output}} = 5\text{v}$. If the LDR is in total lighting, its resistance tends towards zero, so $V_{\text{output}} = 0\text{v}$.

The control card will consist of a microcontroller with an analogue/digital converter which will convert each analogue voltage of output into 8 bits digital code. So values between 0 and 1023 are 1023 for 5 v (total darkness) and 0 for 0 v (total lighting). The sensor tracking method will be detailed in the flowchart.

7.2. The Tilt Axis. The role of the tilt axis is to correct the solar tilt during the year; it can vary between -23.45° at the winter solstice and +23.45° at the summer solstice passing through the 0° at equinox. So an upward and downward variation of 46.9° for one year. According to Figure 22, this axis will also use a worm reducer in addition to a straight pinion reducer. As long as the reduction ratio is increased, the precision increases. The variation of the solar tilt angle is given by Equation (1), but if we want more precision, we can use Equation (8) which gives more precision than Eq. (1) [17].

$$\begin{aligned}\delta = {} & (0.006918 - 0.399912\ \cos\ \Gamma + 0.070257\ \sin\ \Gamma \\ & - 0.006758\ \cos\ 2\Gamma + 0.000907\ \sin\ 2\Gamma \\ & - 0.002697\ \cos\ 3\Gamma + \ \ 0.00148\ \sin\ 3\Gamma) \times (180/\pi),\end{aligned} \quad (8)$$

with $\Gamma = 2\pi(d_n - 1)/365$ In rad or $\Gamma = 360°(d_n - 1)/365$ In degree.

And d_n the number of the day of the year has 1 for February 1 and 365 for December 31. Estimates δ with a maximum error of 0.0006 rad ($<3'$) or if the final two terms are omitted, with a maximum error of 0.0035 rad ($12'$) [17]. Since the variation of the tilt angle is done only once a day, we will use an open-loop variation. That is, the system will correct the tilt axis only once a day at the sunrise. So this axis

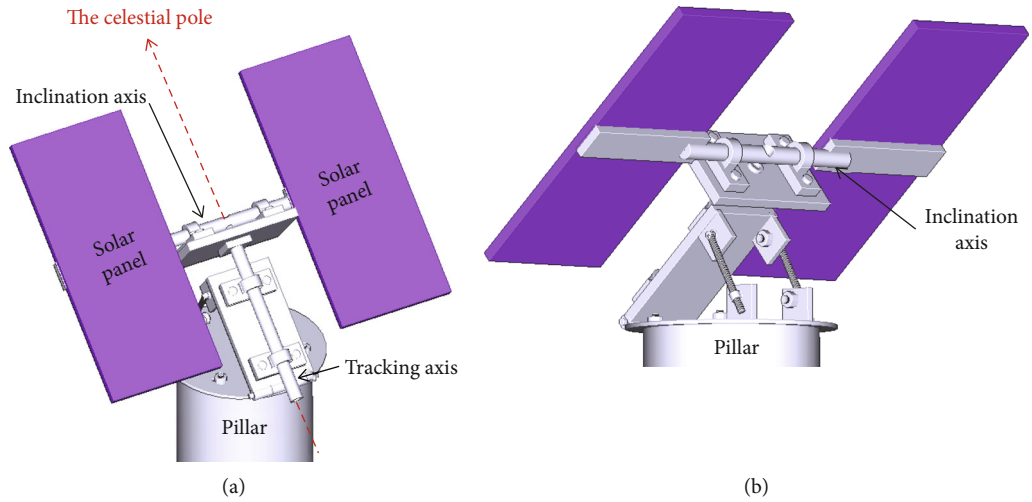

Figure 16: The model of our solar tracker. (a) The solar tracker forward. (b) The solar tracker behind.

Figure 17: The realized model of solar tracker.

will only be functional for a few seconds at the start of the day, thus giving high precision to follow-up while keeping system consumption focused on the engine of the tracking axis. After sunset, we will put the panel in parking mode (Figure 32). This mode consists of making the horizontal panel oriented towards the zenith.

At sunrise, the system must adjust its tilt. Equation (8) allows us to calculate the solar inclination of the day relative to the celestial equator as shown in Figure 11. Now and according to Figure 33, we must put the panel at the proper inclination with respect to the zenith and not with respect to the celestial equator (the panel is oriented to the zenith since it is in parking mode).

In parking mode, the panel is oriented towards the zenith. The angle between the zenith and the polar axis is 90°–Ø (Ø is the latitude of the place as shown in Figure 33). According to Figure 33, we know that the polar axis is perpendicular to the equatorial plane, so the angle between the celestial equator and the polar axis is 90°. So the solar declination at the zenith δz is the angle between the celestial equator and the zenith which equals $\delta z = 90^\circ - (90^\circ - \varnothing) = +\varnothing$.

On leaving parking mode and in order to put the panel facing the sun, the system must activate the tilt motor by an angle (A) between Ø -23.45° (between the zenith and the tropic of cancer) and Ø +23.45° (between the zenith and the tropic of Capricorn). So if we take the zenith as the starting axis and according to Equation (8), the A angel is calculated by the relation:

$$\begin{aligned} A = \varnothing - \delta = (&0.006918 - 0.399912\ \cos\ \Gamma\, 0.070257\ \sin\ \Gamma \\ &- 0.006758\ \cos\ 2\Gamma + 0.000907\ \sin\ 2\Gamma \\ &- 0.002697\ \cos\ 3\Gamma + 0.00148\ \sin\ 3\Gamma) \times (180/\pi), \end{aligned} \tag{9}$$

with $\Gamma = 360^\circ(d_n - 1)/365$ In degree.

The reduction gear used is of the same type as that of the tracking axis with a reduction ratio of $R = 1/6000$. In other words, you have to turn the motor at the reducer inlet at 6000° to have 1° at the outlet. The motor equation is

$$\begin{aligned} A_{\text{mot}} &= A \times 1/R = (\varnothing - \delta) \times 6000 \\ &= [\varnothing[(0.006918 - 0.399912\ \cos\ \Gamma \\ &\quad + 0.070257\ \sin\ \Gamma \quad - 0.006758\ \cos\ 2\Gamma \\ &\quad + 0.000907\ \sin\ 2\Gamma - 0.002697\ \cos\ 3\Gamma \\ &\quad + 0.00148\ \sin\ 3\Gamma) \times (180/\pi)]] \times 6000, \end{aligned} \tag{10}$$

with $\Gamma = 360^\circ(d_n - 1)/365$ In degree.

8. The Control Card

8.1. The Diagram of the Control Card. Figure 34 presents the diagram of the control card with an output of 2 motors, tracking motor (Motor1) and tilt motor (Motor2). The card presents 5 inputs:

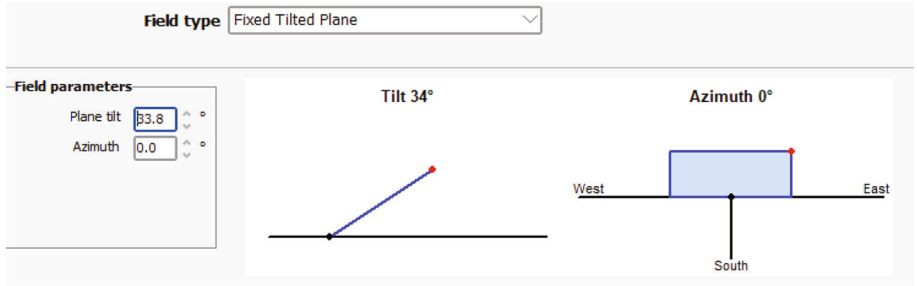

Figure 18: The orientation of the PV in fixed mode.

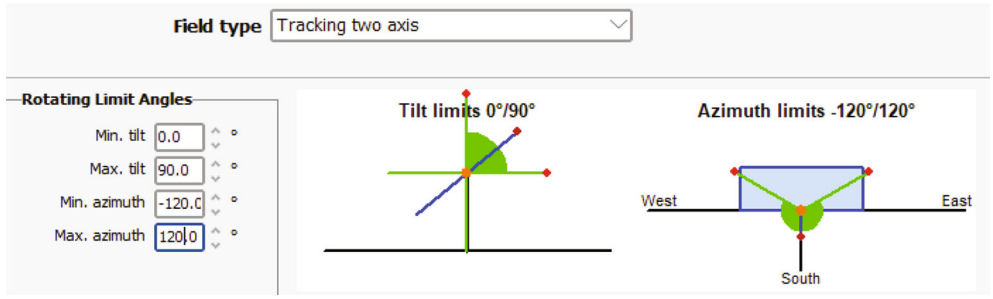

Figure 19: Horizontal and vertical dual-axis solar tracker.

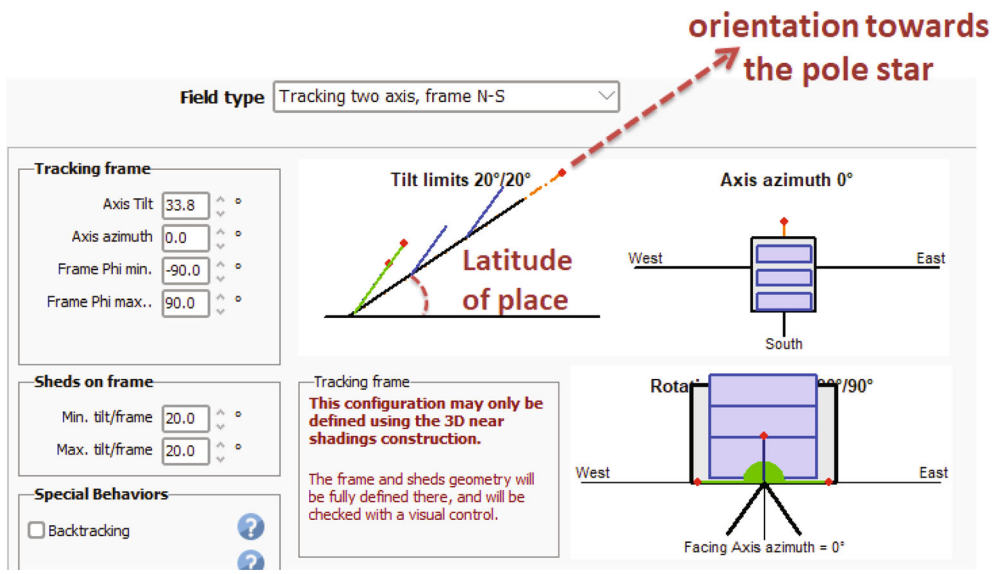

Figure 20: Equatorial biaxial solar tracker model (the proposed model).

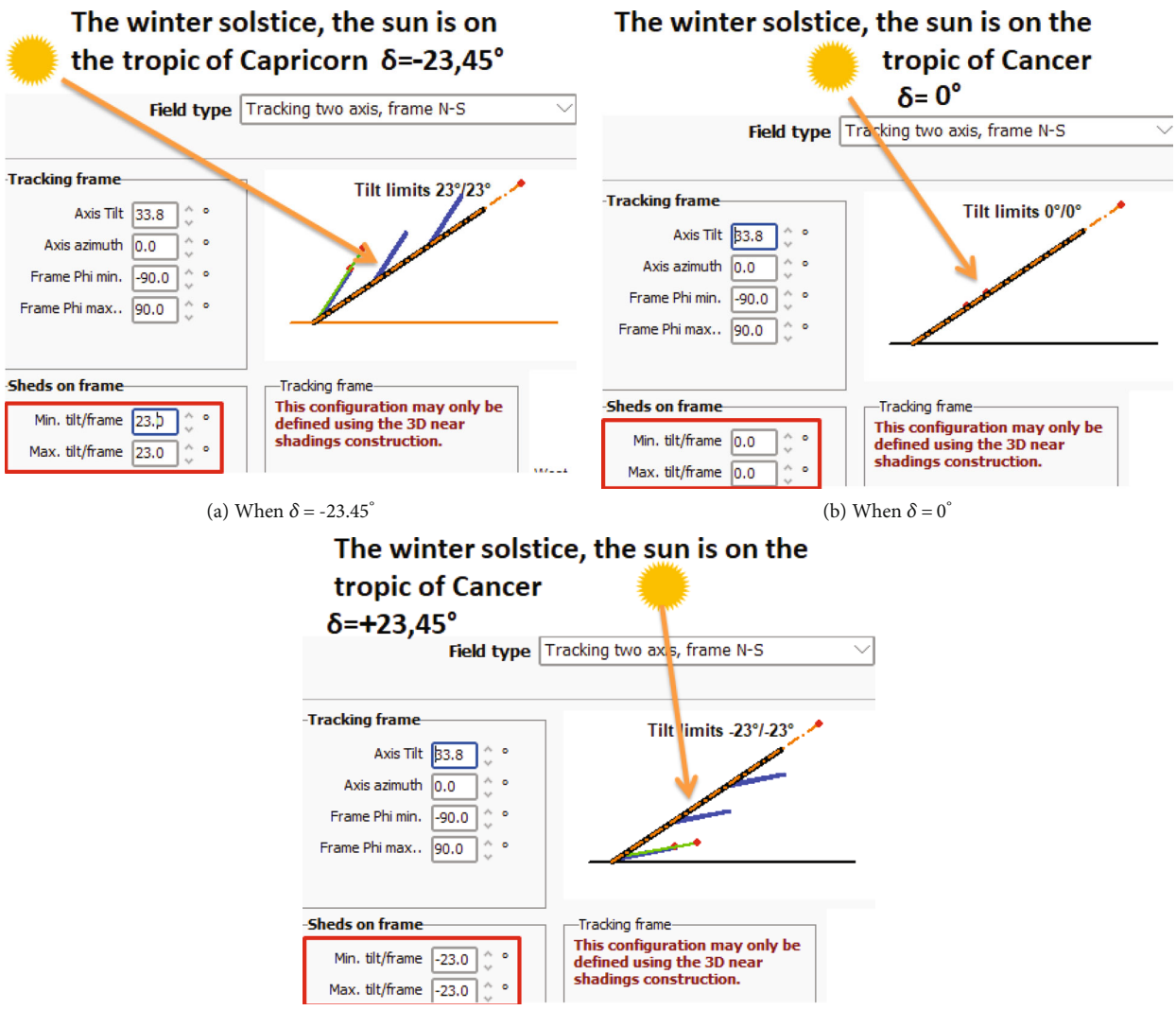

(a) When $\delta = -23.45^{\circ}$

(b) When $\delta = 0^{\circ}$

(c) When $\delta = +23.45^{\circ}$

Figure 21: The tilt of the panel in relation to the solar tilt in PVSYST.

The solar collector: the three analogue signals recovered from the solar collector (Vldr1, Vldr2, and Vldr3) as shown in Figure 31.

B_T *tilt parking brake:* a brake installed on the tilt axis indicates that the panel is in the horizontal position or not (the tilt parking) as shown in Figures 35 and 36.

$B_T = 1$: the panel is in tilt parking mode.

$B_T = 0$: the panel is in nonparking tilt mode.

B_{eq} *equatorial parking brake:* a brake installed on the equatorial axis (tracking axis) indicates that the panel is oriented towards the meridian or not (parking in equatorial) as shown in Figures 37 and 38.

$B_{eq} = 1$: The panel is in equatorial parking mode.

$B_{eq} = 0$: The panel is not in equatorial parking mode.

Wind sensor: in order to avoid damage to the mechanical structure of the solar tracker following the increase in wind speed, we will install an Anemometer to measure the wind speed if it exceeds a set value (wind strong), the system must put the panel in parking mode to avoid any risk. Once the speed drops from the set value, the system resumes tracking. In the algorithm, the set value will be predeclared at the start of the program via a variable, in this way we will be able to change it according to the resistivity of our mechanism (Figure 39).

Clock: in order to calculate and adjust the tilt angle of our solar tracker, we will use an external clock (for example, the DC1307 module). After sunrise or when leaving parking mode, the orientation of the equatorial axis is determined by the sensor, while the orientation of the tilt axis is determined by calculation. This clock gives us the precise date of the day which allows the control card to calculate via Equation (10); the suitable tilt angle is therefore adjusted by the tilt axis. This manipulation will be detailed in the chapter of the organization chart.

8.2. The Organization Chart. According to Figures 40 and 41, the proposed organization chart is divided into 5 principal units:

Table 1: The results of the spring simulation.

Period	δ (°)	Fixed panel (kWh/m^2)	2 axis tracking (kWh/m^2)	Equ. tracking (kWh/m^2)	Gain (%)
20 to 22 Mar	0	20,52	26,38	26,38	28,56
23 to 24 Mar	1	8,76	10,9	10,9	24,43
25 to 27 Mar	2	19,48	24,92	24,92	27,93
28 to 29 Mar	3	13,03	17,05	17,05	30,85
30 Mar to 01 Apr	4	16,46	19,28	19,28	17,13
02 to 03 Apr	5	4,06	4,44	4,44	9,36
04 to 06 Apr	6	20,92	27,11	27,11	29,59
07 to 08 Apr	7	14,7	19,54	19,54	32,93
09 to 11 Apr	8	23,25	31,76	31,76	36,60
12 to 14 Apr	9	23,11	31,57	31,57	36,61
15 to 16 Apr	10	13,27	17,58	17,58	32,48
17 to 19 Apr	11	23,2	32,22	32,22	38,88
20 to 22 Apr.	12	11,41	16,91	16,91	48,20
23 to 25 Apr.	13	19,13	27,66	27,66	44,59
26 to 28 Apr.	14	17,11	22,95	22,95	34,13
29 Apr. to 01 May	15	15	20,91	20,91	39,40
02 to 05 May	16	29,32	40,67	40,67	38,71
06 to 08 May	17	22,6	31,59	31,59	39,78
09 to 12 May	18	21,43	28,59	28,59	33,41
13 to 17 May	19	31,99	46,72	46,72	46,05
18 to 21 May	20	28,33	40,85	40,85	44,19
22 to 27 May	21	42,18	62,35	62,35	47,82
28 May to 03 Jun	22	45,88	66,71	66,71	45,40
04 Jun to 20 Jun	23	64,95	84,75	84,34	29,85
Total		550,09	753,41	753	36,89

Table 2: The results of the summer simulation.

Period	δ (°)	Fixed panel (kWh/m^2)	2 axis tracking (kWh/m^2)	Equ. tracking (kWh/m^2)	Gain (%)
21 Jun. to 06 July	23	176,15	287,65	287,96	63,47
07 to 14 July	22	55,21	80,13	80,13	45,14
15 to 19 July	21	37,55	57,67	57,67	53,58
20 to 24 July	20	36,03	49,51	49,51	37,41
25 to 28 July	19	29,59	42,56	42,57	43,87
29 July to 01 Aug.	18	27,37	39,74	39,75	45,23
02 to 05 Aug.	17	29,37	39,64	39,64	34,97
06 to 08 Aug.	16	23,07	33,9	33,91	46,99
09 to 11 Aug.	15	22,4	32,06	32,07	43,17
12 to 14 Aug.	14	22,82	32,79	32,8	43,73
15 to 17 Aug.	13	22,89	32,87	32,88	43,64
18 to 20 Aug.	12	22,51	31,36	31,37	39,36
21 to 23 Aug.	11	22,35	30,76	30,77	37,67
24 to 26 Aug.	10	21,66	28,53	28,54	31,76
27 to 28 Aug.	9	9,54	12,53	12,53	31,34
29 to 31 Aug.	8	20,52	27,81	27,81	35,53
01 to 03 Sep	7	20,61	26,78	26,79	29,99
04 to 05 Sep	6	15,09	20,57	20,58	36,38
06 to 08 Sep	5	21,16	27,49	27,5	29,96
09 to 10 Sep	4	15,23	20,84	20,85	36,90
11 to 13 Sep	3	22,61	30,48	30,49	34,85
14 to 15 Sep	2	14,49	19,49	19,49	34,51
16 to 18 Sep	1	19,25	25,05	25,06	30,18
19 to 20 Sep	0	8,51	10,2	10,19	19,74
Total		715,98	1040,41	1040,86	45,38

Table 3: The results of the autumn simulation.

Period	δ (°)	Fixed panel (kWh/m^2)	2 axis tracking (kWh/m^2)	Equ. tracking (kWh/m^2)	Gain (%)
21 to 23 Sep	-1	15,53	19,49	19,48	25,43
24 to 25 Sep	-2	13,23	16,95	16,95	28,12
26 to 28 Sep	-3	9,73	10,97	11,01	13,16
29 to 30 Sep	-4	12,74	15,52	15,53	21,90
01 to 03 Oct	-5	15,06	19,04	19,04	26,43
04 to 05 Oct	-6	14,85	19,56	19,57	31,78
06 to 08 Oct	-7	19,69	24,91	24,92	26,56
09 to 11 Oct	-8	19,83	24,62	24,62	24,16
12 to 13 Oct	-9	11,28	13,48	13,48	19,50
14 to 16 Oct	-10	15,64	19,33	19,31	23,47
17 to 19 Oct	-11	20,57	26,19	26,2	27,37
20 to 22 Oct	-12	20,24	26,13	26,14	29,15
23 to 25 Oct	-13	13,19	15,97	15,95	20,92
26 to 28 Oct	-14	20,15	26,17	26,18	29,93
29 to 31 Oct	-15	19,85	25,46	25,47	28,31
01 to 03 Nov	-16	19,87	25,56	25,57	28,69
04 to 07 Nov	-17	25,53	32,48	32,49	27,26
08 to 11 Nov	-18	24,27	30,33	30,34	25,01
12 to 15 Nov	-19	24,79	31,4	31,4	26,66
16 to 20 Nov	-20	23,46	28,94	28,94	23,36
21 to 25 Nov	-21	20,34	25,41	25,39	24,83
26 Nov to 03 Dec	-22	39,41	51,17	51,18	29,87
04 Dec to 21 Dec	-23	17,99	20,83	21,19	17,79
Total		437,24	549,91	550,35	25,87

Table 4: The results of the winter simulation.

Period	δ (°)	Fixed panel (kWh/m^2)	2 axis tracking (kWh/m^2)	Equ. tracking (kWh/m^2)	Gain (%)
22 Dec to 06 Jan	-23	32,53	42,7	42,58	30,89
07 to 13 Jan	-22	42,55	55,71	55,73	30,98
14 to 19 Jan	-21	34,13	45,52	45,53	33,40
20 to 23 Jan	-20	26,95	36,29	36,31	34,73
24 to 28 Jan	-19	23,61	30,03	30,02	27,15
29 Jan to 01 Feb	-18	27,44	36,48	36,5	33,02
02 to 04 Feb	-17	12,78	16,26	16,25	27,15
05 to 08 Feb	-16	22,88	29,6	29,59	29,33
09 to 11 Feb	-15	19,03	25,12	25,12	32,00
12 to 14 Feb	-14	16,55	21,69	21,69	31,06
15 to 17 Feb	-13	21,82	28,37	28,38	30,06
18 to 20 Feb	-12	21,98	28,6	28,61	30,16
21 to 23 Feb	-11	22,5	29,52	29,53	31,24
24 to 25 Feb	-10	14,34	18,43	18,44	28,59
26 to 28 Feb	-9	20,7	26,28	26,29	27,00
01 to 02 Mar	-8	11,67	13,82	13,82	18,42
03 to 04 Mar	-7	8,77	10,28	10,28	17,22
05 to 07 Mar	-6	11,09	14,05	14,05	26,69
08 to 09 Mar	-5	9,79	11,83	11,83	20,84
10 to 12 Mar	-4	10,79	13,26	13,26	22,89
13 to 14 Mar	-3	8,61	10,92	10,93	26,95
15 to 17 Mar	-2	14,32	16,73	16,73	16,83
18 to 19 Mar	-1	9,05	11,97	11,97	32,27
Total		443,88	573,46	573,44	29,19

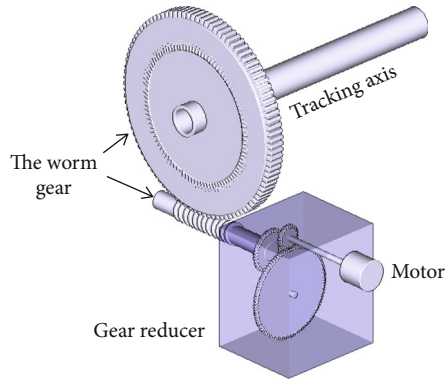

Figure 22: Worm wheel type reducer with a pinion reducer.

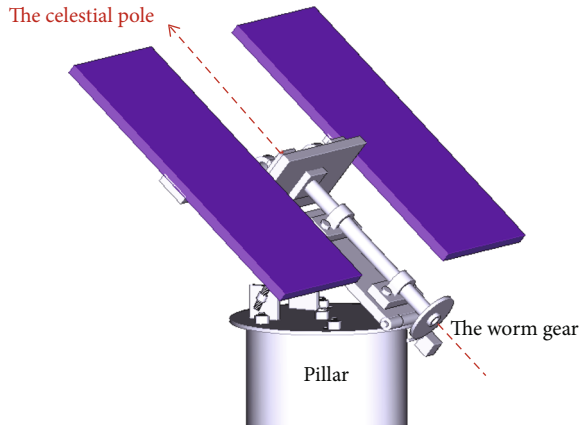

Figure 23: The motorization of the tracking axis.

Start-up unit: declaration of used variables and preparation for system start-up.

The program needs 6 variables to be created: 3 variables of 8 bits $\boldsymbol{x}$, $\boldsymbol{y}$, and $\boldsymbol{M1}$, one variable of 1-bit **parking** (we will explain later the detailed use of each of these variables).

Then, the test system two inputs B_T and B_{eq} (the inclination and equatorial brakes as shown in Figures 34–38); if they are both at 1, the panel is in the parking position. The system actually starts; otherwise (both of them at 0), we have to orient the panel manually so that it is in parking mode (this is a manipulation that is done once during the installation of the tracker).

Core unit of the program: specify the operating mode of the solar tracker according to the sky condition (night mode, cloudy day mode, and clear sky day mode).

After the system starts up, the program enters the main loop (infinite loop).

We will start with the wind speed test given by a wind sensor installed on the mechanism as shown in Figures 34 and 39; if it exceeds a predefined value, the system switches to parking mode. This value will be set on the program.

If the wind test is favourable, the system links the analogue inputs from the solar sensor LDR1 and LDR2, then converts them into digital code (between 0 and 1023), and stocks them, respectively, on the 8 bits variables $\boldsymbol{x}$ and $\boldsymbol{y}$.

Thereafter, we will test its values if they are all greater than 1000 (value per experience). If yes, that is to say, that the 2 DLRs are in total darkness and, then, we are at night, the solar tracker goes into parking mode.

If not, that is to say, that we are in day mode. We will do a second test of these variables, if they are all greater than 800 (value per experience); if yes, that is to say, that we are in day mode with overcast sky, the system back to the beginning of "core of the program" block. In order to reduce energy consumption, the follower is in stop mode.

If not we are in daylight mode, the system actually begins the correction. We do a second wind test before starting the correction. If the test is favourable, go to the tilt adjustment.

Tilt adjustment unit: the system must put the panel at an angle suitable for that of the sun through the tilt axis. This manipulation is done only once at the start of each day or when leaving parking mode.

We start with the test of the variable "parking" which determines whether the follower in parking mode or not.

If "parking = 0," we exceed this block (the follower is already in good inclination).

If "parking = 1," then the tracker is in parking mode. The system retrieves the number of the day from an external clock module (DC1307).

Then, according to Equation (10), the system calculates the number of turns that the tilt motor must make. Finally, the tilt motor 2 is activated at the top in order to put the panel in a suitable tilt. Before leaving the block, the system set the parking variable to 0 (so as not to repeat the loop the next time).

Lighted sky unit (orientation towards the sun): if the program arrives at this stage, that is to say, that it is in daylight mode. This loop puts the panel in orientation towards the sun through the equatorial axis.

We start by rereading and converting the LDR values of the solar collector ($\boldsymbol{x}$ = LDR1, $\boldsymbol{y}$ = LDR2).

Then, we will make a digital comparison between $\boldsymbol{x}$ and $\boldsymbol{y}$ (a comparison between the voltage recovered from LDR1 and LDR2).

If $\boldsymbol{x} > \boldsymbol{y}$, the motor 1 is actuated in WEST (the sun is west of the solar tracker) and does not stop unless $\boldsymbol{x} = \boldsymbol{y}$. During this movement, each time, the wind speed must be tested and the LDR1 and LDR2 read again.

If $\boldsymbol{x} < \boldsymbol{z}$, the motor 1 is actuated in EAST (the sun is east of the solar tracker) and does not stop unless $\boldsymbol{x} = \boldsymbol{y}$. During this movement, each time, the wind speed must be tested and the LDR1 and LDR2 read again.

If $\boldsymbol{x} = \boldsymbol{y}$, we must stop the correction and return to the beginning of the program.

$\boldsymbol{M1}$ is a variable that indicates the location of the panel to the east or west relative to the meridian as shown in Figure 42. If the motor 1 is activated in the east, we will put $\boldsymbol{M1}$ in 1; if the motor 1 is activated in the west, we will put $\boldsymbol{M1}$ in 2. The state of this variable will be necessary to make the panel in parking mode.

Parking unit as shown in Figure 41: this mode consists of putting the horizontal panel facing the zenith as shown in Figure 32 in two cases:

(1) After sunset

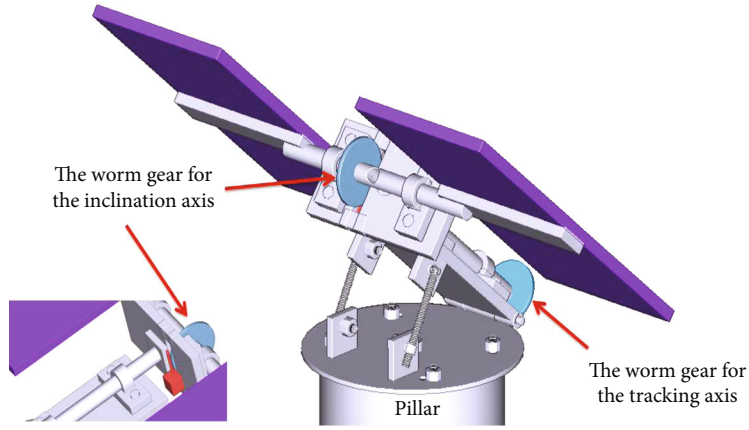

Figure 24: The motorization of the tracking axis.

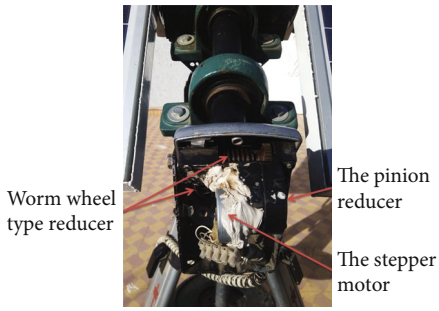

Figure 25: The type reducer "DiseqC motor" with a stepper motor.

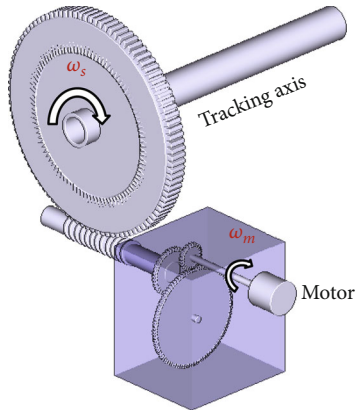

Figure 26: The rotation speed of the tracking motor.

(2) In case the wind speed exceeds a threshold, so as not to damage the structure

The **Parking** variable informs us about the state of the mechanism whether it is in parking mode or not. So at the start, we will test this variable if it is 1, the mechanism is in parking mode, and then, we will leave the loop. If **Par king = 0**, then the system is not in parking mode; we will start by putting the tilt axis in parking. Normally, the tilt axis in nonparking mode is always at the top of the horizon as shown in Figure 33, so just lower the panel via the actuation of motor 2 at the bottom. If the mechanism touches the tilt brake ($B_T = 1$), the panel is therefore in parking in tilt.

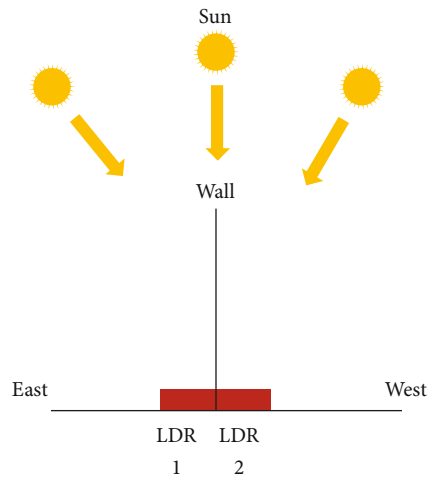

Figure 27: The diagram of the proposed solar collector.

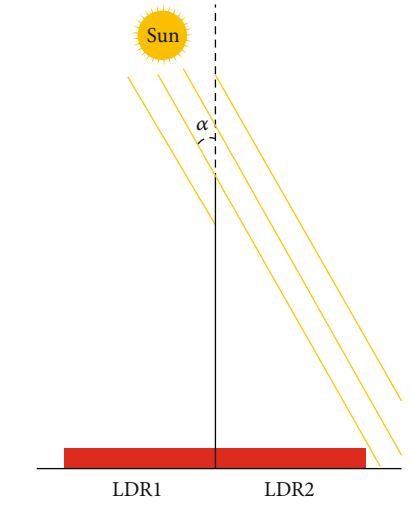

Figure 28: The length of the LDR sensor wall.

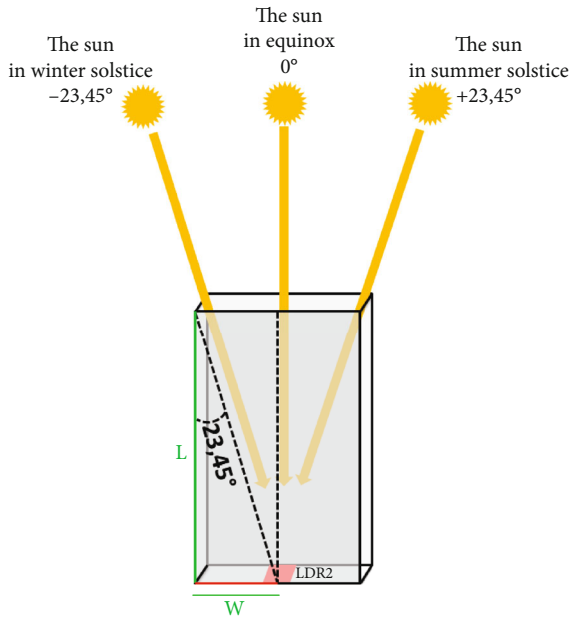

Figure 29: The width of the solar collector wall.

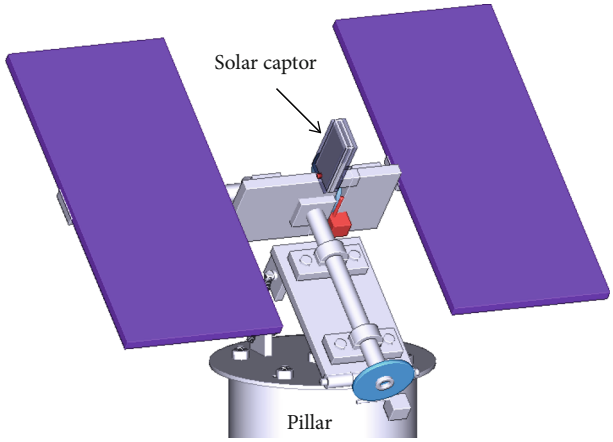

Figure 30: The solar tracker model with solar collector.

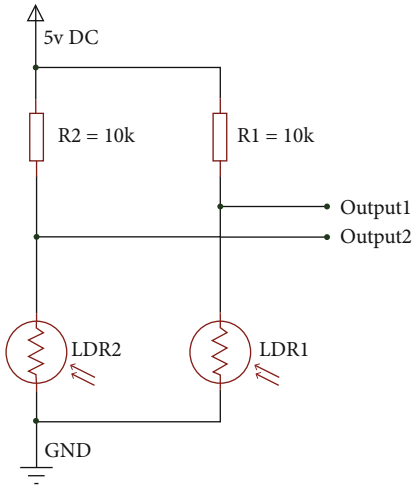

Figure 31: The electronic diagram of the solar captor.

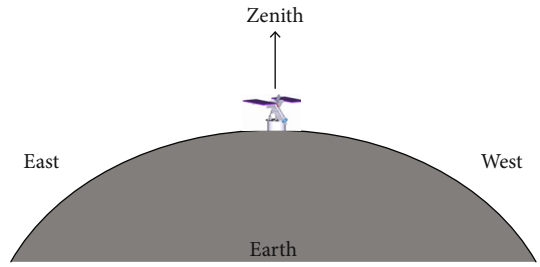

Figure 32: The panel is oriented towards the zenith.

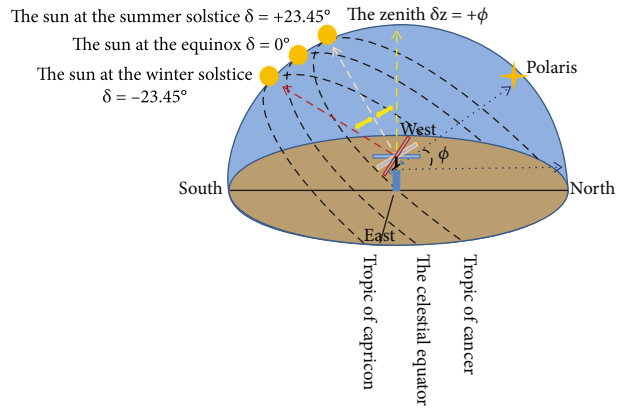

Figure 33: Panel tilt adjustment after the parking mode.

Then, we go to the equatorial axis, the variable ***M*1** variable tells us whether the panel is located in east or west relative to the meridian. If ***M*1** = **1**, the panel is in east relative to the meridian; we must activate motor 1 in west. If ***M*1** = **2**, the panel is in west compared to the meridian we must activate the motor 1 in east. If ***M*1** = **0**, the panel is parked on an equatorial axis (the panel is oriented at the meridian).

As motor 1 turns, the system tests the equatorial brake B_{eq}, if $B_{eq} = 1$, so we are in parking mode in equatorial, motor 1 stops. Before leaving the loop, we put the variable ***M*1** in 0.

Note: in programming, the blocks on the flowchart colored in verse will be treated as interruptions.

8.3. The Realisation of the Control Card. According to Figure 43, the microcontroller used is of the PIC16F877A type which will drive the two stepper motors via the ULN2304 circuit.

(i) The 4 buttons B1, B2, B3, and B4 are intended to activate the two motors manually (task necessary in order to put the panel in parking mode when the system is started).

B1 = Motor 1 in west/B2 = Motor 1 in east.
B3 = Motor 2 at the top/B4 = Motor 2 at the bottom.

(ii) The wind sensor will be connected to RB0/INT, which is an interrupt on the microcontroller

(iii) The solar collector will be connected to the connectors of the analogue-to-digital converters RA0/AN0, RA1/AN1, and RA2/AN2

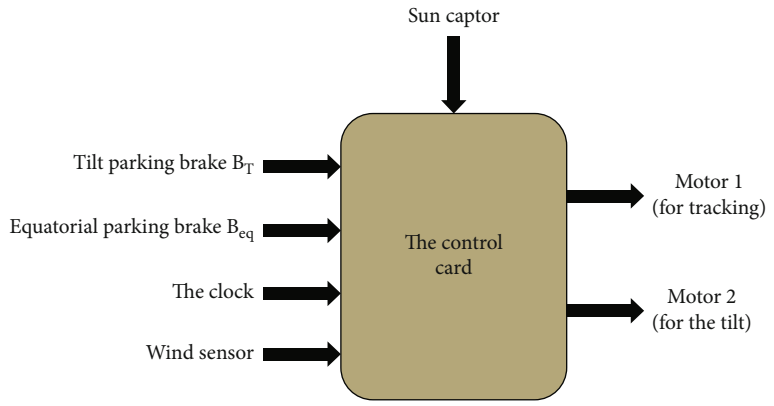

Figure 34: The diagram of the control card.

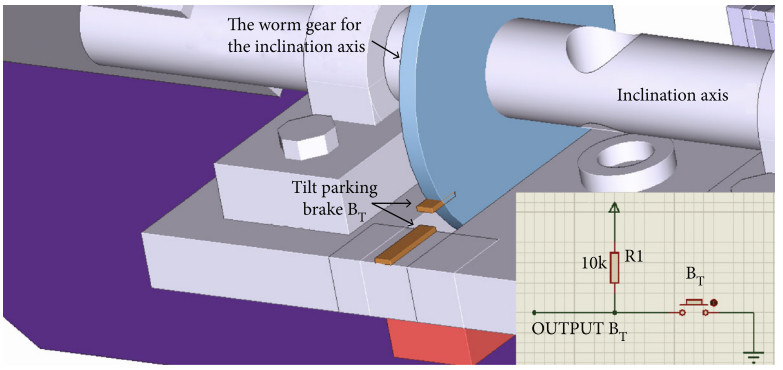

Figure 35: The tilt parking brake B_T.

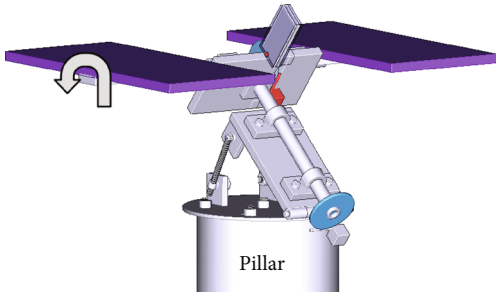

Figure 36: The solar tracker in the tilt parking position.

(iv) The DC1307 clock module will be connected via the I2C bus of the microcontroller (RC3/CSL and RC4/SDA)

(v) The analogue-to-digital inputs will be dedicated to the solar sensor (LDR1 = RA0, LDR2 = RA1, and LDR3 = RA2)

(vi) The tilt axis brake B_T and the equatorial axis brake B_{eq} will be connected, respectively, to the branches RB4 and RB5 (interrupt on the microcontroller)

(vii) The clock used is of the PSTN DS1307 type and will be connected to the microcontroller via the I2C bus (RC3 and RC4)

(viii) The motors chosen are unipolar stepper motors 55SI-25DAYA

(ix) The microcontroller drives the two motors via the power circuit ULN2804

(x) We are going to add an LCD screen like (LCD HD44790 16 x 2) in order to visualize the state of the tracker (the mode of our solar tracker, time, date, and the movement of the motors)

9. Experience and Results

9.1. The Production. On September 26, 2020, in Khemisset city (latitude = 33.8°), we have made an experiment of two solar panels with the same characteristics. The first panel was in a fixed mode (oriented towards the south and inclined at an angle equal to latitude of the location), while the second was in a tracking mode. At noon, we reversed the panels to ensure symmetry between both configurations (Figure 44). The characteristics of the solar panels are: $V_{co} = 22.1\ V$, $V_{mpp} = 18.2\ V$, $I_{cc} = 2.95\ A$, $I_{mpp} = 2.75\ A$.

So the form factor is So

$$FF = \frac{(V_{mpp} \times I_{mpp})}{(V_{co} \times I_{cc})} = \frac{P_{mpp}}{(V_{co} \times I_{cc})} = 0.76.$$
$$P_{mpp=}0,76 \times (V_{co} \times I_{cc}). \quad (11)$$

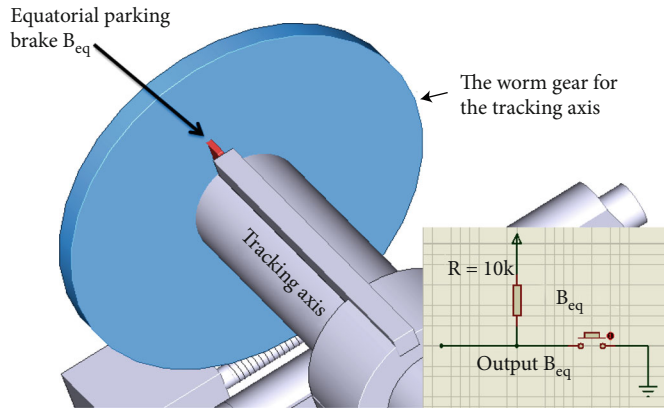

Figure 37: Equatorial parking brake B_{eq}.

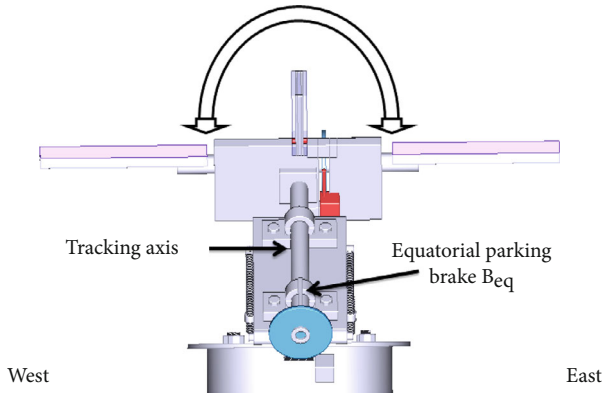

Figure 38: The solar tracker in the equatorial parking position.

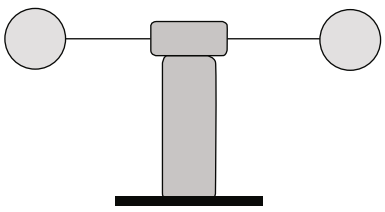

Figure 39: Anemometer.

We measured every 30 min the V_{co} and I_{cc} to calculate the power of each photovoltaic panel using Equation (11). The obtained results are shown in Table 5 and graph (Figure 45).

Based on the results above, it was observed that solar panels productivity has been increased by 37% in motion mode compared to fixed mode.

Based on simulation results of September, the gain in percentage of the quantity of irradiation received by a surface using our proposed model is about 30% compared to a fixed installation, which is approximately equal to the experience results.

9.2. The Consumption. The tracking motor: at sunrise, the panel is in parking mode (towards the zenith); the system orients the panel to the east in order to prepare it for the sunrise. So the system travels 90° to the east.

During the day, the system makes a tracking from sunrise to sunset, by making a total of 180° course.

However, after sunset, another 90° course in the opposite direction is achieved in order to make the panel in parking position (towards the zenith).

So the system in general makes a 360° during 24 hours; this trip lasts on average T1 = 49 min 20 sec. So the electrical energy consumed by the system (the tracking motor plus the control card) is

$$\begin{aligned} P_1 &= P_{\text{control board(c.b.)}} + P_{\text{tracking motor(tr.m.)}} \\ &= (V_{\text{c.b.}} \times I_{\text{c.b.}}) + (V_{\text{tr.m.}} \times I_{\text{tr.m.}}) \\ &= (5\text{V} \times 0.1) + (12\text{V} \times 0.13\text{A}) \\ &= 2.06\text{W}. \end{aligned} \tag{12}$$

N.B.: motor and control card voltage and current are measured experimentally.

The tilt motor: the day of the experiment on September 26 (d_n=270), the angle that the tilt motor must make is 55° (calculated according to the Equation (9)). So at sunset, the tilt motor lies 55° degrees up and 55° down at sunset; it is a 110° course. By measurement, this course last T2 = 15 min 20 sec, and the current measured between the terminals of the motor is 0.145 A. So the electrical energy consumed by the system (the tilt motor plus the control board) is

$$\begin{aligned} P_2 &= P_{\text{control board(c.b.)}} + P_{\text{tilt motor(ti.m.)}} \\ &= (V_{\text{c.b.}} \times I_{\text{c.b.}}) + (V_{\text{ti.m.}} \times I_{\text{ti.m.}}) \\ &= (5\text{V} \times 0.1) + (12\text{V} \times 0.145\text{A}) \\ &= 1.74\text{W}. \end{aligned} \tag{13}$$

N.B.: motor and control card voltage and current are measured experimentally.

When the motors stopped (tilt motor or tracking motor), the power consumption of the control board measured is

$$P_3 = P_{\text{control board}} = (5\text{V} \times 0.1) = 0.5\text{W (by measure)}. \tag{14}$$

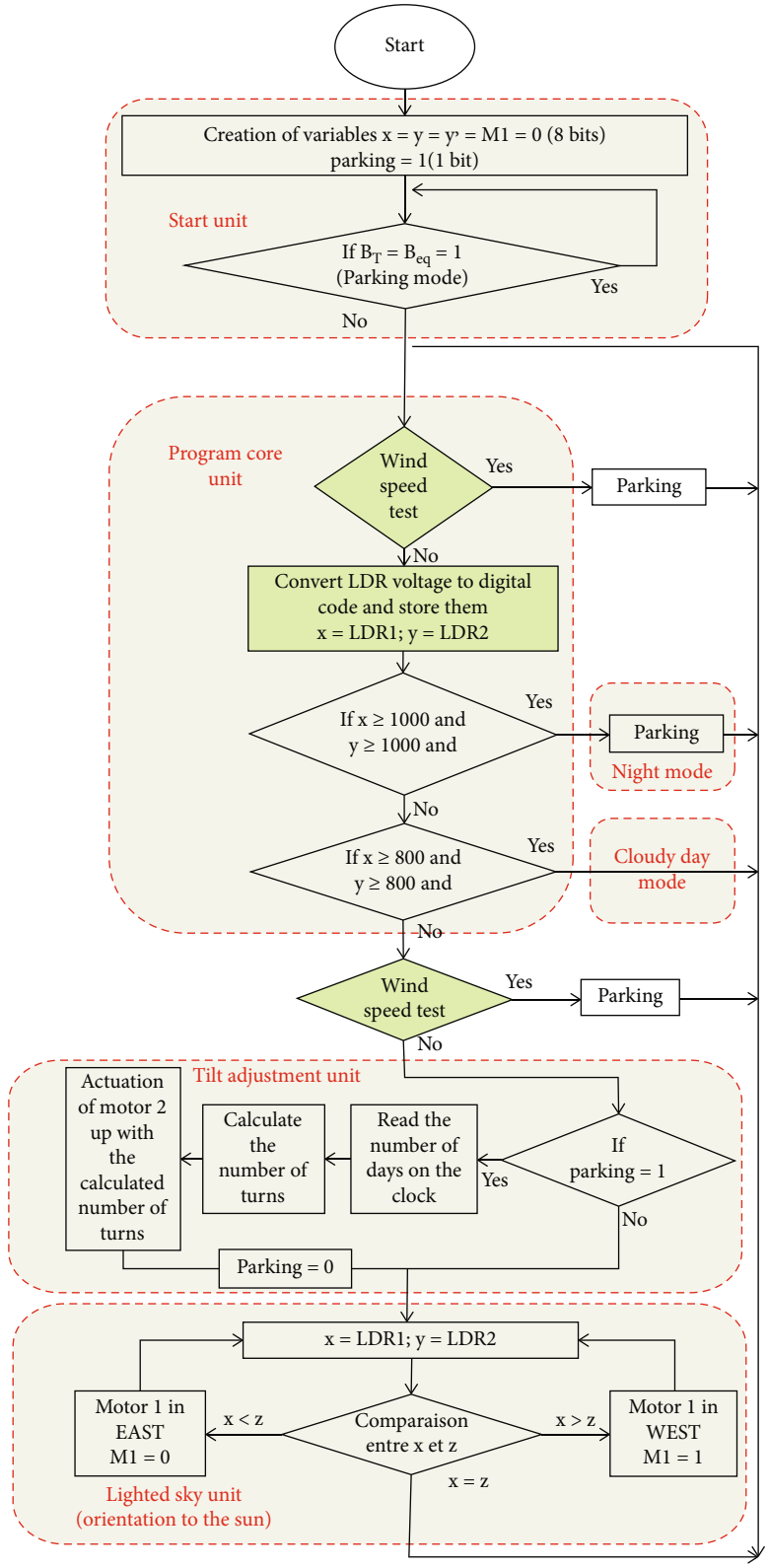

Figure 40: The principal flowchart.

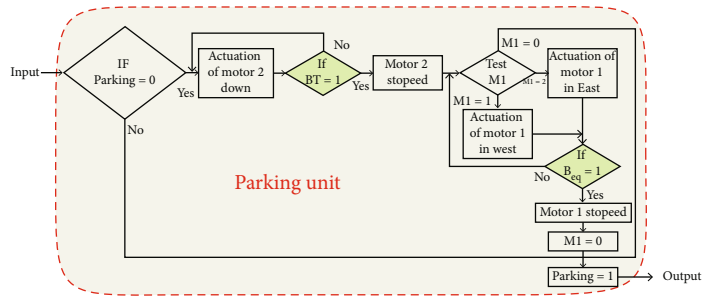

Figure 41: The flowchart of the parking unit.

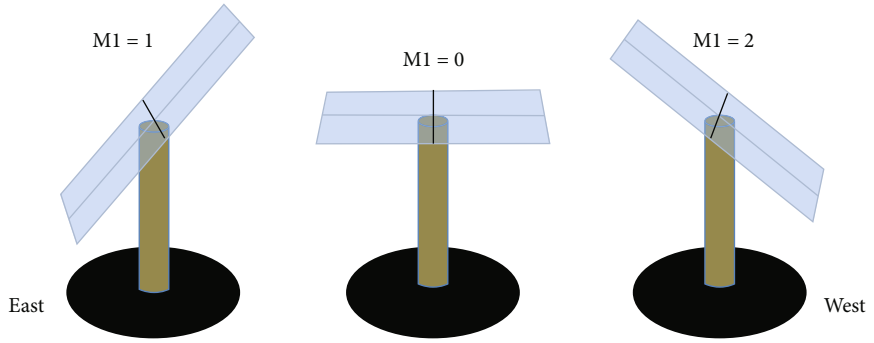

Figure 42: The state of variable M1.

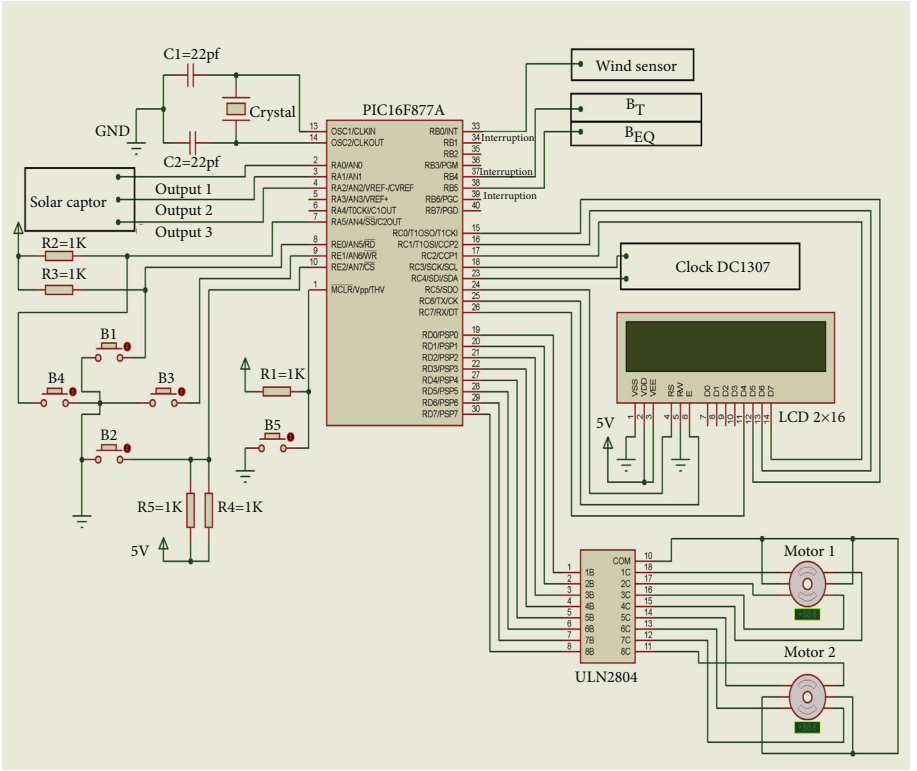

Figure 43: Diagram of the control board.

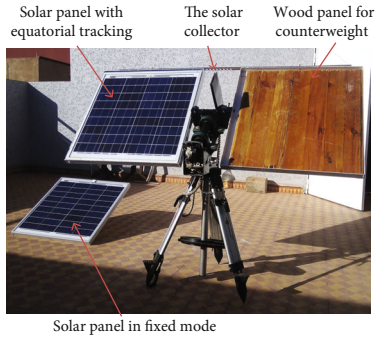

Figure 44: The solar panel on the right in the tracking mode, the one on the left in the fixed mode.

The control board is always on, so P_3 is the power consumption of the board at an equal duration T3 = 24 h-T1-T2 = 1375 min 20 sec (the rest of the day).

So the power consumed (P) for 24 hours is

$$P = \left(P_1 \times \frac{T_1}{T_1 + T_2 + T_3}\right) + \left(P_2 \times \frac{T_2}{T_1 + T_2 + T_3}\right) + \left(P_3 \times \frac{T_3}{T_1 + T_2 + T_3}\right) = 41.26\text{W}. \quad (15)$$

9.3. The Cost of the Concept. According to Table 6, this cost remains reasonable by comparing it with those of other embodiments, for example, the cost of the prototype proposed by the publication [9, 12].

Each tracking system will surely have drawbacks; the drawback of this system is the duration that the mechanism puts during the orientation of the panel to the east after sunset (25 min), and this is actually due to the use of a stepper motor which is a precision but not fast motor compared to a DC motor. The use of a DC motor requires the addition of a pitch encoder to specify tracking. It should also be remembered that the use of a DC motor increases system consumption.

10. Conclusion

In order to minimize the consumption of a solar tracker while keeping its accuracy to the maximum, we have proposed a concept based on the equatorial mount. The concept of the proposed system is that the majority of the tracker consumption is focused on the equatorial motor which gives us a significant minimization of energy dissipated during the follow-up.

In order to valorize our model, we made a comparison simulating three modes of installation of photovoltaic panel: the 1st in fixed mode, the 2nd in biaxial azimuthal tracking mode, and the 3rd in two-axis equatorial tracking mode (the proposed model). The results showed us that a panel mounted on a biaxial equatorial tracker receives the maximum amount of solar irradiation compared to other tracking modes. The simulation also showed us that with our model, we will have a solar irradiation gain of up to 63.47% compared to a panel in fixed mode and an annual average of 35.71%.

Table 5: The results of the experiment.

Hour	The results of the fixed panel			The results of the moving panel		
	I_{cc} (A)	V_{co} (V)	P_{mpp} (W)	I_{cc} (A)	V_{co} (V)	P_{mpp} (W)
06 : 30	0,06	17	0,78	0,24	19,3	3,52
07 : 00	0,28	18,4	3,92	1,1	20,9	17,47
07 : 30	0,51	20	7,75	1,51	20,8	23,87
08 : 00	1,02	20,5	15,89	2,49	20,6	38,98
08 : 30	1,46	20,	22,86	2,78	20,5	43,31
09 : 00	1,98	20,7	31,15	3,11	20,5	48,45
09 : 30	2,36	20,5	36,77	3,19	20,2	48,97
10 : 00	2,65	20,6	41,49	3,24	20,3	49,99
10 : 30	2,92	20,5	45,49	3,3	20,3	50,91
11 : 00	3,16	20,4	48,99	3,36	20,2	51,58
11 : 30	3,26	20,2	50,05	3,36	20,2	51,58
12 : 00	3,3	20,2	50,66	3,35	20,2	51,43
12 : 30	3,31	20,4	51,32	3,37	20,3	51,99
13 : 00	3,22	20,4	49,92	3,33	20,5	51,88
13 : 30	3,12	20,2	47,90	3,31	20,2	50,82
14 : 00	2,96	20,6	46,34	3,28	20,5	51,10
14 : 30	2,74	20,7	43,11	3,26	20,6	51,04
15 : 00	2,44	20,6	38,20	3,23	20,5	50,32
15 : 30	2,07	20,6	32,41	3,15	20,6	49,32
16 : 00	1,63	20,6	25,52	2,97	20,7	46,72
16 : 30	1,21	20,4	18,76	2,72	20,7	42,79
17 : 00	0,7	20,1	10,69	2,43	20,9	38,60
17 : 30	0,4	19,6	5,96	1,6	20,8	25,29
18 : 00	0,03	15,9	0,36	0,33	19,3	4,84
18 : 30	0	13,2	0,00	0,02	13,8	0,21
	Total		726,28	Total		995,00

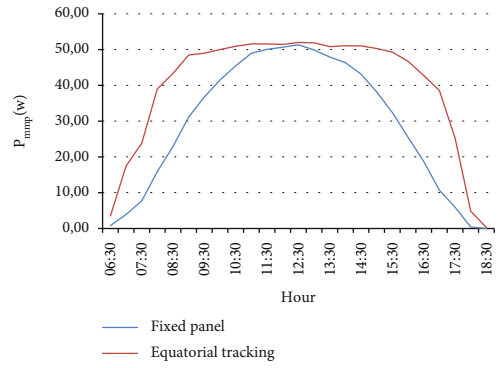

Figure 45: The comparison between a fixed solar panel and that in motion.

After having carried out the project, and in order to experimentally validate these results, we have proceeded to the real test experimentation which consists in making a comparison of the electrical energy produced by a PV panel using fixed mode and the one using equatorial tracking

Table 6: Cost of different components of the proposed concept.

Material	Number of material	Unit cost ($)	Total cost ($)
The stepper motor 55SI-25DAYA	2	6.5	13
The reducer of DiseqC motor	2	38	76
The structure of the equatorial mount	1	38	38
The control card and the solar captor	1	9	9
TOTAL			136

mode. The measurement obtained during the test allows us to conclude that our solar tracking system consumes less energy with a high accuracy.

11. Perspective

The proposed model based on a monoaxial equatorial tracking, plus a daily tilt correction, and since the solar tilt changes from the tropic of Capricorn (winter solstice), to the concert tropic (summer solstice) passing through the equinox and in order to validate and generalize the results of the new concept, we will work on the possibility of carrying out these experiments spread over a minimum period of six months, between the spring equinox and the autumn equinox. We will also measure the actual consumption of our solar tracker over this period, thus providing an overall assessment of our model.

Data Availability

No data were used to support this study.

Conflicts of Interest

The authors declare that they have no conflicts of interest.

Authors' Contributions

Hicham Bouzakri, as the corresponding author, designed the equatorial solar tracker model with all the descriptions mentioned in the document, plus the realization of the prototype. Ahmad Abbou supervised the written paper and provided the necessary data. Khalil Tijani has contributed to the simulation via PVsys. Khalil Tijani and Zakaria Abousserhane have contributed to the writing and the paper organization. All authors approved the final version. The authors declare no conflict of interest.

References

[1] S. R. Wenham, M. A. Green, M. E. Watt, and R. Corkish, *Applied Photovoltaics*, Earthscan, 2007.

[2] Z. Abousserhane, A. Abbou, L. Id-Khajine, and N. E. Zakzouk, "Power flow control of PV system featuring on-grid and off-grid modes," in *2019 7th International Renewable and Sustainable Energy Conference (IRSEC)*, pp. 1–7, Agadir, Morocco, 2019.

[3] Y. Zhu, J. Liu, and X. Yang, "Design and performance analysis of a solar tracking system with a novel single-axis tracking structure to maximize energy collection," *Applied Energy*, vol. 264, article 114647, 2020.

[4] R. Bayindir, E. Kabalci, H. I. Bülbül, and C. Can, "Optimization of operating conditions of photovoltaic systems: a case study," in *2012 International Conference on Renewable Energy Research and Applications (ICRERA)*, pp. 1–4, Nagasaki, Japan, 2012.

[5] A. Ponniran, A. Hashim, and H. Ali Munir, "A design of single axis sun tracking system," in *2011 5th International Power Engineering and Optimization Conference*, pp. 107–110,, Shah Alam, Selangor, 2011.

[6] L.-V. Oon, M.-H. Tan, C.-W. Wong, and K.-K. Chong, "Optimization study of solar farm layout for concentrator photovoltaic system on azimuth-elevation sun-tracker," *Solar Energy*, vol. 204, pp. 726–737, 2020.

[7] R. Eke and A. Senturk, "Performance comparison of a double-axis sun tracking versus fixed PV system," *Solar Energy*, vol. 86, no. 9, pp. 2665–2672, 2012.

[8] R. Shaik, N. Beemkumar, H. Adharsha, K. Venkadeshwaran, and A. D. Dhass, "Efficiency enhancement in a PV operated solar pump by effective design of VFD and tracking system," *Materials Today: Proceedings*, vol. 33, pp. 454–462, 2020.

[9] H. Fathabadi, "Novel high efficient offline sensorless dual-axis solar tracker for using in photovoltaic systems and solar concentrators," *Renewable Energy*, vol. 95, pp. 485–494, 2016.

[10] Z. Mi, J. Chen, N. Chen, Y. Bai, R. Fu, and H. Liu, "Open-loop solar tracking strategy for high concentrating photovoltaic systems using variable tracking frequency," *Energy Conversion and Management*, vol. 117, pp. 142–149, 2016.

[11] C. Jamroen, P. Komkum, S. Kohsri, W. Himananto, S. Panupintu, and S. Unkat, "A low-cost dual-axis solar tracking system based on digital logic design: design and implementation," *Sustainable Energy Technologies and Assessments*, vol. 37, article 100618, 2020.

[12] H. Fathabadi, "Novel high accurate sensorless dual-axis solar tracking system controlled by maximum power point tracking unit of photovoltaic systems," *Applied Energy*, vol. 173, pp. 448–459, 2016.

[13] A. Awasthi, A. K. Shukla, S. R. Murali Manohar et al., "Review on sun tracking technology in solar PV system," *Energy Reports*, vol. 6, pp. 392–405, 2020.

[14] H. Bouzakri and A. Abbou, "Study and realization of a mono-axial solar tracker over an equatorial mount," in *2019 7th International Renewable and Sustainable Energy Conference (IRSEC)*, pp. 1–6, Agadir, Morocco, 2019.

[15] H. Bouzakri and A. Abbou, "Mono-axial solar tracker with equatorial mount, for an improved model of a photovoltaic panel," *International Journal of Renewable Energy Research*, vol. 10, no. 2, pp. 578–590, 2020.

[16] R. Berry, *Build Your Own Telescope*, Willmann-Bell, New York, NY, USA, 3rd edition, 2001.

[17] M. Iqbal, *An Introduction to Solar Radiation*, Elsevier, 1983.